

Efficient and Diverse Generative Robot Designs using Evolution and Intrinsic Motivation

Leni K. Le Goff¹ and Simón C. Smith¹

Abstract—Methods for generative design of robot physical configurations can automatically find optimal and innovative solutions for challenging tasks in complex environments. The vast search-space includes the physical design-space and the controller parameter-space, making it a challenging problem in machine learning and optimisation in general. Evolutionary algorithms (EAs) have shown promising results in generating robot designs via gradient-free optimisation. Morpho-evolution with learning (MEL) uses EAs to concurrently generate robot designs and learn the optimal parameters of the controllers. Two main issues prevent MEL from scaling to higher complexity tasks: computational cost and premature convergence to sub-optimal designs. To address these issues, we propose combining morpho-evolution with intrinsic motivations. Intrinsically motivated behaviour arises from embodiment and simple learning rules without external guidance. We use a homeokinetic controller that generates exploratory behaviour in a few seconds with reduced knowledge of the robot’s design. Homeokinesis replaces costly learning phases, reducing computational time and favouring diversity, preventing premature convergence. We compare our approach with current MEL methods in several downstream tasks. The generated designs score higher in all the tasks, are more diverse, and are quickly generated compared to morpho-evolution with static parameters.

I. INTRODUCTION

The physical configuration of a robot, including its body, limbs, sensors and actuators, plays a crucial role in its capacity to solve any task. In domains where no robotic solution exists, experts can develop a robot, including its physical design and training of its controller. As another solution, generative artificial intelligence automatically designs robots and their controllers, accelerating the production of innovative digital and physical artefacts [1], [2]. Examples of generative design applied to robotics include the use of reinforcement learning (RL) [3], [4], topology optimisation [5] and evolutionary algorithms (EAs) [6], [7], [8], [9]. While RL and topology optimisation are limited to gradient-based design-spaces, gradient-free methods such as EAs offer more flexibility. The generation of robot designs using artificial evolution, *morpho-evolution*, results in innovative configurations of actuators, sensors and passive parts able to solve complex tasks in dynamic environments. Examples of morpho-evolution include soft robotics [10], [11], fine-tuning of existing designs [12] and the generation of a diverse set of high-performing designs [6].

Classic morpho-evolution algorithms consider the solution-space as the joint space of the robot designs and controller parameters. Usually, these algorithms use EAs

for robots design optimisation [13], [14], [15]. However, these works study linear tasks in a reduced solutions-space, and the results are not applicable to physical robots. The design-space only includes proprioception and a reduced set of actuators, leaving out external sensors or actuators like manipulators.

To scale morpho-evolution to more complex tasks and larger design-spaces integrating exteroception, the methods require a learning phase [16], [6], [7]. These approaches combine learning and morpho-evolution. First, an Evolutionary Computation (EC) algorithm generates robot designs, and a second process optimises the parameters of the controller for each design. In this paper, we refer to this framework as *morpho-evolution with learning* (MEL).

Two main issues prevent MEL from tackling higher-complexity tasks. First, applying a learning phase to each design results in a high computational cost [17]. For instance, authors in [6] can generate diverse designs by combining deep RL and morpho-evolution. However, the approach requires a large computational power (1152 CPUs). Luo et al. [17] compares morpho-evolution and MEL approaches, showing that with the same computational power, classic morpho-evolution (without learning) was able to run 200 generations while MEL was still at its first generation.

Second, the studies [18], [10], [11] show that MEL framework suffers from premature convergence, resulting in locally optimal solutions reducing the diversity of possible designs. The authors in [11] show that the learning processes accentuate the premature convergence by comparing learning against a controller with static parameters, i.e. fixed controller. With a fixed controller, the diversity of design is higher than using a learning algorithm. This study is limited to distributed controller with only proprioceptive sensors.

To address these issues, we propose to integrate intrinsic motivation with morpho-evolution to efficiently generate optimal and diverse designs. Intrinsically motivated (IM) robots can behave in exploratory or curious ways without external rewards [19]. The IM behaviour emerges from the robot’s embodiment and internal representations of the world and its dynamics. Algorithms for IMs usually operate with fast online adaptation rather than lengthy learning phases. A robot without prior knowledge of the world’s or its own dynamics starts exploring the environment in a few seconds. IMs in robotics include guided RL, theories for internal model self-organisation, and automatic curriculum learning [20], [21], [22], [23]. Compared to MEL’s learning phase, our approach can quickly decide if a design is viable by checking its IM behaviour. In this way, thousands of

¹School of Computing, Engineering & The Built Environment, Edinburgh Napier University, UK. l.legoff2@napier.ac.uk, s.smith2@napier.ac.uk

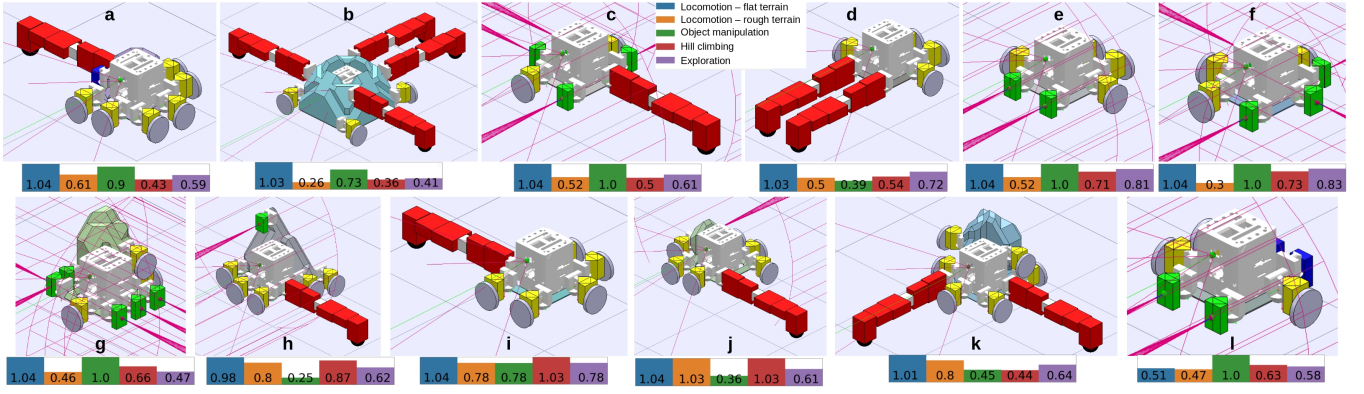


Fig. 1. Robots generated by our approach MEHK. Exploration values refer to the evaluation phase during morpho-evolution. The other values correspond to the downstream task scores.

robots can be generated and evaluated in significantly less time than current MEL approaches.

To the best of our knowledge, only [24] proposes a similar approach, task-agnostic morphology evolution (TAME). The authors combine morpho-evolution with empowerment [25]. They show that empowerment is a good proxy for viable robot designs that generalise to multiple tasks. However, empowerment requires an accurate model of the dynamics between the robot and the environment. This model can be acquired as prior knowledge or learned during training. This last approach is inefficient for dynamic environments and requires an extensive data set for each robot.

We propose to combine morpho-evolution with *homeokinesis* (MEHK). Homeokinesis generates seemingly intelligent exploratory behaviour by adapting the controller's parameters in linear time by maximising predictability and sensitivity [26]. Homeokinesis replaces the lengthy learning process in MEL, e.g. RL, CMA-ES or EAs, required to test each generated design, with a short adaptation period that is able to make a robot move in an exploratory way in a few seconds of simulation. MEHK calculates a fitness function as coverage of the environment. In this case, homeokinesis is a proxy towards optimal designs, filtering designs unsuitable for movement or interaction with the environment. To test MEHK, we train the generated solutions in several downstream tasks. We select the best robots from a Pareto front between fitness and design diversity. We compare MEHK to a baseline of robots generated with morpho-evolution with a fixed controller.

Our contributions are: (1) introducing homeokinesis to the generative robotic design framework, including exteroceptive sensors; (2) introducing MEHK as a fast method for generating a high number of robot designs with low computational resources; and (3), we show that the solutions found by MEHK have higher performance for downstream tasks when compared to a morpho-evolution with a fixed controller.

II. METHODOLOGY

A. Morpho-Evolution with Homeokinesis (MEHK)

a) Morpho-evolution: Our method is based on the Asynchronous Morpho-Evolution (AME) algorithm [27].

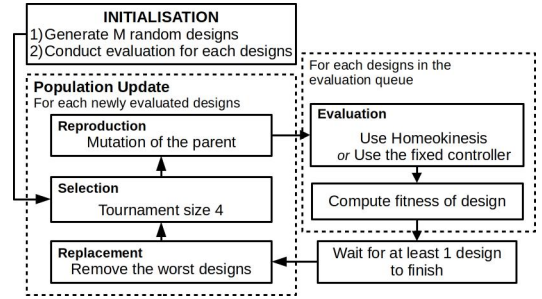


Fig. 2. Asynchronous Morpho-Evolution. Our approach, MEHK, uses intrinsically motivated behaviour, homeokinesis, for evaluation.

AME works on two sets: a population and an evaluation queue (Fig. 2). The population is the set of robot designs already evaluated and ready for reproduction. The evaluation queue is the set of newly generated designs waiting to be evaluated. The initial population include 100 designs produced by a randomly generated *compositional pattern-producing network* for each design [28] (CPPN, more details in Sec. II-C).

At each iteration, the algorithm updates the population. Each robot design, i.e. solution or individual, is evaluated to assess their quality by calculating its fitness. In MEHK, fitness is the coverage of the robot over the environment while it is controlled by homeokinesis for 20 minutes. As MEHK is an asynchronous EA, the population is updated as soon as a design is evaluated. This update has three steps:

Replacement: The newly evaluated designs are added to the population, and the same number of designs are removed, keeping the population size constant. The designs with the lowest fitness are removed.

Selection: The selection is done with a tournament. Four designs are randomly selected from the population, and the one with the highest fitness is selected for reproduction.

Reproduction: The topology, weights and activation functions of the CPPN that generated the selected parent are mutated. The neurons of the CPPN can have 4 activation functions: Gaussian, sigmoid, sinusoid, or linear. The weights and activation function parameters are modified with polynomial mutation. A forward pass of the CPPN generates a new solution.

b) Homeokinetic Controller: Homeokinesis (HK) is a principle that generates coordinated and seemingly intelligent behaviour without specific goals [26]. The robot's behaviour fluctuates between *predictability* and *sensitivity*. Predictable behaviours are the ones that result in a change in the state of the robot that can be predicted by an internal forward model. At the same time, sensitive behaviour is the one where a small action produces a significant change in the state of the robot. HK defines a controller C , an internal forward model M and a sensorimotor loop Ψ , with sensors s and actuators a :

$$\begin{aligned} a_t &= C(s_t), \\ \tilde{s}_{t+1} &= M(s_t, a_t), \\ \Psi(s_t) &= M(s_t, C(s_t)). \end{aligned}$$

We can define the prediction error E at time t , and the Jacobian matrix L as:

$$\begin{aligned} E_t &= \|s_t - \tilde{s}_t\|, \\ L_{ij} &= \frac{\partial \Psi_i}{\partial s_j}. \end{aligned}$$

Thus, the time-loop error, TLE , is defined as,

$$TLE_t = \|L_t^{-1} E_t\|^2. \quad (1)$$

The controller parameters are updated to minimise the TLE , and the forward model is updated to minimise E . This definition of the TLE assumes that an inverse of L exists¹. Following Eq. 1, we can see that the learning rule favours predictable behaviour by minimising E , i.e. behaviours that M predicts more accurately. At the same time, the learning rule favours sensitive behaviour by minimising the inverse of L , i.e. behaviours that have a larger impact on the dynamics. The result is exploratory behaviour that quickly adapts to excite all the robot's degrees of freedom while maintaining control and being reactive to external perturbations.

c) Baseline: Morpho-Evolution with Fixed Controller (MEFC): As a baseline, MEHK is compared to AME with a fixed controller for design evaluation (Fig. 2). The controller is a feed-forward neural network with one hidden layer of 6 neurons. The number of inputs and outputs depends on the robot design (Fig. 3). At the beginning of an evaluation, MEFC draws weights and bias values from a uniform distribution in the interval $[-0.5, 0.5]$.

B. Learning Algorithm for the Downstream Tasks

As a final step of the experiments, a selection of robots generated by MEHK are trained on a set of tasks (Sec. III). The learning algorithm used is a variant of *covariance matrix adaptation evolutionary strategies* (CMA-ES) augmented with novelty (NCMA-ES) [29]. CMA-ES is a population-based optimisation algorithm using a multivariate normal distribution to sample solutions. In our case, the solution is the parameters of an Elman network used to control the robot.

¹To calculate L , an input shift η is applied to the sensorimotor loop as $\Psi(s_t + \eta_t) = \tilde{s}_{t+1} + E_{t+1}$, and a Taylor expansion to obtain a new form for $E_{t+1} = L_t \eta_t$

NCMA-ES has two objectives: the task score (fitness value or reward) and the novelty score. The novelty score measures how much a behaviour obtained from a solution is novel compared to the current population and past solutions. Both objectives are combined in a weighted sum. The weights are initialised to 1 for the novelty score and 0 for the task score. At each iteration, the weights are decreased and increased by the same increment (0.05 in our experiments). NCMA-ES progressively transitions from a pure novelty search process to a pure goal-based optimisation process.

C. Robotic design space

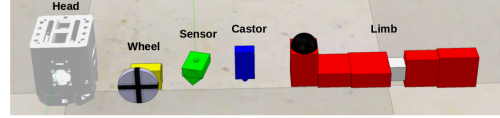


Fig. 3. Five components for the robot's design.

a) Design-space: The robotic design-space follows the ARE project [30], [31]. A robot comprises 5 pre-designed components assembled on a free-formed voxel-based chassis (Fig. 3). The chassis is limited to a matrix of voxels of $11 \times 11 \times 11$.

The *head* is the central computing unit of the robots². The *head* is always in the middle-bottom body of the robots. A maximum of 8 components can be fixed on the surface of the chassis. There are 4 different components: limbs, wheels, sensors and castors. A limb has two degrees of freedom: one rotating on a horizontal axis and one rotating on a vertical axis. Each proximity sensor includes an infrared (IR) receiver. The proximity sensor outputs a continuous value between 0 and 1 as the distance to the closest object, and the IR receiver outputs a binary value when an object emitting IR light is detected.

b) Controller: The controller representation depends of which algorithm is used.

For MEHK, homeokinesis uses a pseudo-linear controller. The next action is calculated as $a_{t+1} = g(Cs_t + c)$, where g is a sigmoidal activation function, C an $m \times n$ matrix (m the number of actuators, and n the number of sensors), and c a bias term. The homeokinetic forward model is defined in action-space as $\tilde{s}_{t+1} = Aa_t + b$, where A is an $n \times m$ matrix and b is a bias term. The controller's parameters are updated with a stochastic gradient descent algorithm over the TLE error and the model over the prediction error E .

For MEFC, the fixed controller is a feed-forward neural network, and NCMA-ES optimises the parameters of an Elman network to learn the downstream tasks. Both networks have 6 hidden neurons.

For the three controllers, the input includes the angular positions of each wheel, the angular positions of each joint (2 per limb), the proximity sensor value bounded in $[0, 1]$, and IR receiver value equal to 0 or 1. The outputs are converted

²On the physical robot, the head is composed of a battery, Raspberry Pi and custom PCBs.

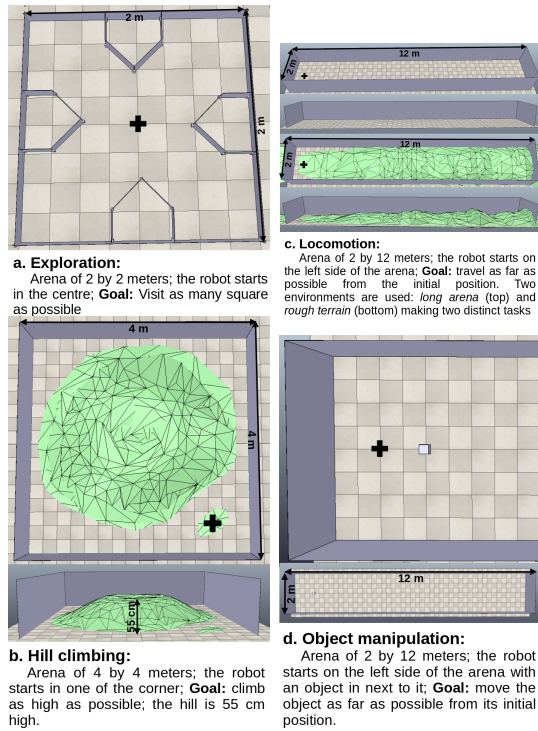


Fig. 4. **a)** Arena used for the evaluation of the robots during MEHK generative phase. **b), c)** and **d)**, are the downstream tasks environments. For clarity, **d)** only shows the beginning of the arena.

into target velocity for each wheel or goal position for the joints. For MEFC and NCMA-ES, the outputs for the joints are converted into a frequency of a sinusoidal function before sending it to the robot. The input and output values for the actuators are normalised between $[-1,1]$.

c) Encoding: The *compositional pattern producing network* (CPPN) [28] is used to generate the design of the robots. A CPPN neural network generates spatial patterns using spatial coordinates as inputs. The design is generated based on a 3-dimensional square matrix of size 11. Each voxel of the matrix can be empty, be a piece of the chassis, or be the attached point of one of the four components. The CPPN is queried for each voxel to determine its content. The CPPN has four inputs: x , y , z , and r , corresponding to the 3-dimensional coordinates of the voxel and its distance to the centre of the robot. The network outputs 5 values for each voxel corresponding to each possible component: a piece of chassis, a wheel, a limb, a sensor or a castor. Details of the decoding procedure can be found in [30].

III. EXPERIMENTAL PROTOCOL

To test our approach, we first generate 10000 robot designs with MEHK and MEFC. Then, we select the best design to train them on the downstream tasks. All the experiments are replicated 30 times³.

A. Generation phase

The generation phase consists of running MEHK and MEFC on an *exploration* task: the robots have 20 minutes to

explore as much as possible an environment (Fig. 4a). The arena is divided into a grid of 8×8 cells to compute the exploration fitness score. The score is the number of cells uniquely visited divided by the total number of cells.

This phase generates diverse designs and evaluates their viability. The exploration task biases the designs for functional combinations of actuators, sensors and the shape of the chassis towards embodiment, i.e. robots able to move and interact with the environment.

The budget for each run of MEHK and MEFC is 10000 episodes, and each run of the algorithms generates 10000 designs.

B. Robotic design selection

After the generation phase, 3 designs are selected to be trained to solve the downstream tasks. First, a selection is made by keeping the designs with a fitness value above a set threshold (0.4 for MEHK and 0.2 for MEFC). This selection guarantees a minimum exploratory quality of the designs. Then, a *sparsity score* based on a *morphological descriptor* is computed.

The morphological descriptor is a 3-dimensional square matrix of size 11 representing the design-space. The matrix of integers indicates the type of components located in each voxel. 0 indicates an empty voxel or a piece of chassis, 1 to 4 the presence of a component. To obtain a sparse matrix, the descriptor does not store the chassis, increasing the computational efficiency. Finally, the sparsity score is computed by averaging the Euclidean distance between the design and its 15 nearest neighbours in the descriptor space.

A Pareto front is computed based on the fitness value and sparsity score. Three designs are picked in this front: the two edges of the set, i.e. maximising the fitness value and maximising the sparsity score, and the one at the centre of the set, i.e. having a median value of fitness and sparsity.

C. Downstream Tasks Learning

The 3 selected design are trained on 4 tasks using NCMA-ES.

Hill climbing: Fig. 4b. Starting in one corner of a 4×4 meters arena, the fitness function is the highest altitude the robot reaches after a 120 seconds episode.

Locomotion: Fig. 4c. In this task, the robot starts on the far left of a 12 meter arena and has to travel as far as possible. The fitness function is the distance between the initial and final positions of the robot. Two environments are used for this task: an empty and a rough terrain arena. In the rough arena, the terrain gets incrementally harder to navigate. We separate the tasks into *locomotion-on-flat-terrain* and *locomotion-on-rough-terrain*. The episodes last 240 seconds.

Object manipulation: Fig. 4d. Similar to the locomotion task, the robot starts at the left of an empty arena. A cube of 10cm is placed 50cm in front of the robot. The cube is an IR emitter detectable by the robot sensors. The robot has to move the cube and the fitness function is the

³The code will be available upon acceptance

distance between the initial and final positions of the cube. The episode's length is 240 seconds.

We run NCMA-ES with a budget of 10000 evaluations and a population of 50 controllers.

IV. RESULTS

A. Generation phase

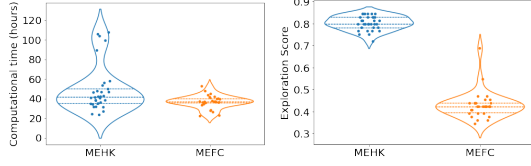


Fig. 5. Comparison of MEHK (blue) and MEFC (orange). On the left, the total computational time and on the right, best exploration score obtained from each replicate.

Fig. 5 shows the distribution of the computational time and the best exploration score of MEHK and MEFC. MEHK outperform MEFC with an exploration score median of 0.8, while MEFC has a median of 0.45. This result shows that homeokinesis is an effective proxy for exploratory behaviour for any closed-loop robot design. In comparison, the fixed controller architecture is only effective when randomly generated parameters align with the robot's dynamics. Except for some outliers for MEHK, both variants use the same computational time with a median of around 40 hours of wall time to generate and evaluate 10000 robots.

Fig. 6 shows the percentage of robots generated with respect to their number of components (filled bars) and their exploration scores (empty boxes). Similarly, Fig. 7 shows the exploration score over chassis depth, height and width, the number of voxels (dots) and a Kernel density estimation for the data (lines). Note that the number of sensors does not include proprioception, which is always present for wheels and limbs. The results show that half of the robots have a peak performance for 2 and 3 sensors, while some robots without sensors also have high performance. MEHK generates a majority of robots with wheels (40% with 4 wheels and 30% with 5 wheels) with the best exploration score. The exploration is maximal for robots with 0 or 1 limb. The score decreases with the increase of limbs. Overall, homeokinesis can efficiently control a diverse range of combinations of components but is less efficient with a larger number of limbs. Note that the placement of the components biases the robot's behaviour, as shown by the spread of the exploration scores for different designs.

MEFC generates a majority of robots with at least 1 limb (95%). 55% of the designs have no wheel and 70% have no sensors. For most of the MEFC robots, the exploration score is comparable, except for lower scores for more than 5 sensors, 5 wheels, or no joints. From these results, we can see that the fixed controller can only exploit robots with joints.

The exploration score is higher for MEHK than for MEFC. The robots generated by MEHK can explore and react to

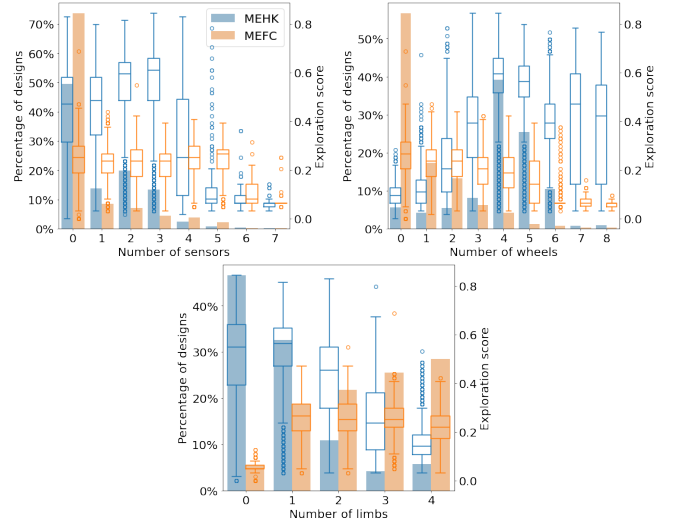


Fig. 6. Percentage of robots with respect to the number of components (filled bars), and their exploration score (empty boxes).

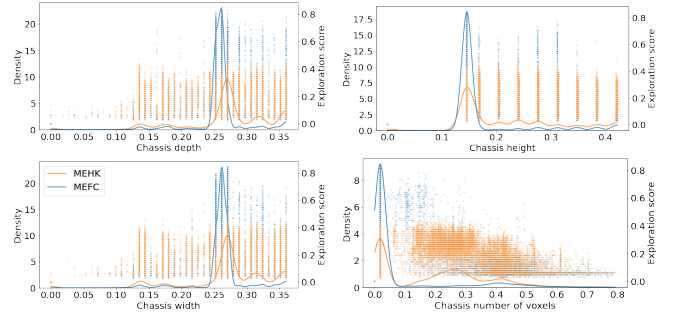


Fig. 7. Exploration scores of each robot (dots) with respect to the dimension and volume of the chassis. The lines represent the density distribution of the data estimated by a KDE algorithm.

the environment more efficiently than the ones generated by MEFC. This result is explained by the nature of the behaviours that HK brings about. In this case, embodiment plays a crucial role in the designs, as the controller can only be as effective as the robot allows. At the same time, the designs evolve to enable homeokinetic behaviour. Also, Fig. 6 shows a more homogeneous distribution of the number of components for the MEHK designs. MEHK can generate a wider diversity of designs than MEFC when comparing components. We believe that the improvement in exploration score and diversity is crucial for the solution of downstream tasks.

MEFC generated a higher diversity of chassis than MEHK, Fig. 7. Most MEHK designs have a small chassis that is enough to hold the head. Considering the exploration score, MEFC has a flatter distribution and is less elitist than MEHK. The bias for small chassis in MEHK makes robots more stable and less prone to falling to the side or turning upside down while exploring. Even with this bias, MEHK generated robots with high exploration scores in a range of chassis.

B. Downstream Tasks

Fig. 8 shows scores obtained by each robot on the downstream tasks. Maximum, median and distribution of the

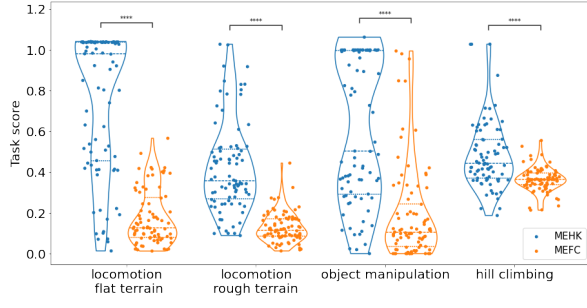


Fig. 8. Best performance scores of each robot for the different tasks. Each dot represents one robot, and the violin plots synthesise the distributions. The four stars above the results indicate a p-value less than 10^{-4} in a Brunner-Munzel statistical test.

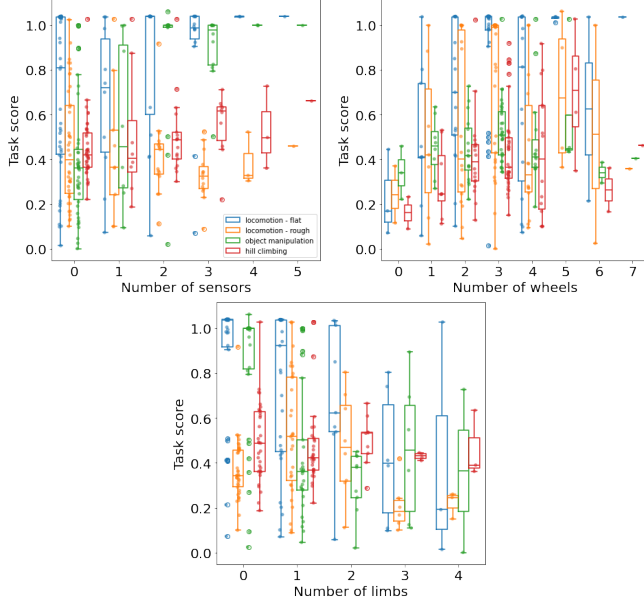


Fig. 9. MEHK results for the 4 tasks over the number of sensors (top left), number of wheels (top right) and the number limbs (bottom).

results show that MEHK solves all the tasks and has higher scores than MEFC. In the flat terrain locomotion task, most MEHK robots reach the end of the arena (score greater or equal to 1). In rough terrain, the median score is close to 0.4, which is a result of more challenging terrain. In both terrains, MEFC shows a lower median and distribution of the score. Fig. 9 shows the task score for the locomotion tasks (blue and orange) over the number of components for MEHK. As expected, on the flat terrain, the best robots have wheels. Also, the best performances are achieved with more sensors due to the ability to avoid obstacles and walls. On rough terrain, the best robots have a combination of one limb and wheels. However, with more than one limb NCMA-ES fails to find a good policy due to higher dimensionality in the search-space and the interaction between the limbs and the terrain.

In the object manipulation task, MEFC scores are similar to the locomotion task except for a longer tail with a few robots able to push the object toward the end of the arena. MEHK results are split into two groups, one with high performance (0.6 or greater) and another with lower

performance (less than 0.5). Fig. 9 shows that most high-performing robots have sensors. The robots can change their behaviour based on the object's position, while robots without sensors operate in an open loop. Similarly to locomotion on flat terrain, the best robots have wheels.

In the hill climbing task, the median for both MEFC and MEHK are similar (around 0.4 and 0.5, respectively). MEHK results have a tail of higher performance. Only three robots from MEHK were able to reach the top of the hill (robots **b** and **i** in Fig. 1). Fig. 9 shows that most combinations of components have a similar distribution, with few outliers. Only robots with 4 or 5 wheels show higher performance.

Finally, Fig. 1 shows examples of high-performing robots generated by MEHK. Robots **b**, **e**, **f**, **h**, and **i** are generalists able to perform well on most tasks. Robots **d**, **g**, **k**, and **l** are specialists that perform well only on 1 or 2 tasks. Moreover, the exploration score (purple in Fig. 1) has minimal impact on the performance of the downstream tasks. In this set of robots, the one with the best performance on all the tasks does not have the best exploration score. Exploration is necessary for a successful robot design in these tasks but is insufficient. Thus, the diversity of solutions generated by MEHK is a crucial component for improved overall performance.

V. DISCUSSION AND CONCLUSIONS

We propose a new algorithm combining morpho-evolution and homeokinesis (MEHK) to generate more efficient and diverse designs in less time than current morpho-evolution approaches. We show that MEHK solutions are viable designs for downstream tasks. MEHK is computationally efficient compared to MEL frameworks. With 64 CPUs, MEHK can generate and evaluate 10000 designs in 40 hours. In comparison, Gupta et al.[6] use MEL with deep reinforcement learning. The authors used 1152 CPUs to generate and evaluate 4000 designs.

The generated designs are biased by the policy used to evaluate them. MEFC generates robots with several joints and diverse chassis shapes, while MEHK generates a large diversity of combinations and configurations of components with smaller chassis. In future work, we are interested in studying the influence of other intrinsic motivation architectures.

ACKNOWLEDGEMENT

This work is funded by Edinburgh Napier University and EPSRC ARE project, EP/R03561X, EP/R035733, EP/R035679.

COPYRIGHT

This work has been submitted to the IEEE for possible publication. Copyright may be transferred without notice, after which this version may no longer be accessible.

REFERENCES

- [1] Z. Epstein, A. Hertzmann, I. of Human Creativity, M. Akten, H. Farid, J. Fjeld, M. R. Frank, M. Groh, L. Herman, N. Leach, *et al.*, “Art and the science of generative ai,” *Science*, vol. 380, no. 6650, pp. 1110–1111, 2023.
- [2] F. Buonamici, M. Carfagni, R. Furferi, Y. Volpe, L. Governi, *et al.*, “Generative design: an explorative study,” *Computer-Aided Design and Applications*, vol. 18, no. 1, pp. 144–155, 2020.
- [3] K. S. Luck, H. B. Amor, and R. Calandra, “Data-efficient co-adaptation of morphology and behaviour with deep reinforcement learning,” in *Conference on Robot Learning*. PMLR, 2020, pp. 854–869.
- [4] M. Li, D. Matthews, and S. Kriegman, “Reinforcement learning for freeform robot design,” in *2024 IEEE International Conference on Robotics and Automation (ICRA)*. IEEE, 2024, pp. 8799–8806.
- [5] D. Matthews, A. Spielberg, D. Rus, S. Kriegman, and J. Bongard, “Efficient automatic design of robots,” *Proceedings of the National Academy of Sciences*, vol. 120, no. 41, p. e2305180120, 2023.
- [6] A. Gupta, S. Savarese, S. Ganguli, and L. Fei-Fei, “Embodied intelligence via learning and evolution,” *Nature communications*, vol. 12, no. 1, p. 5721, 2021.
- [7] L. K. Le Goff, E. Buchanan, E. Hart, A. E. Eiben, W. Li, M. De Carlo, A. F. Winfield, M. F. Hale, R. Woolley, M. Angus, *et al.*, “Morpho evolution with learning using a controller archive as an inheritance mechanism,” *IEEE Transactions on Cognitive and Developmental Systems*, vol. 15, no. 2, pp. 507–517, 2022.
- [8] M. Jelisavcic, K. Glette, E. Haasdijk, and A. Eiben, “Lamarckian evolution of simulated modular robots,” *Frontiers in Robotics and AI*, vol. 6, p. 9, 2019.
- [9] W. Li, E. Buchanan, L. K. Le Goff, E. Hart, M. F. Hale, M. De Carlo, R. Wooley, A. F. Winfield, J. Timmis, and A. M. Tyrrell, “Evaluation of frameworks that combine evolution and learning to design robots in complex morphological spaces,” *IEEE Transactions on Evolutionary Computation*, 2023.
- [10] N. Cheney, J. Bongard, V. SunSpiral, and H. Lipson, “Scalable co-optimization of morphology and control in embodied machines,” *Journal of The Royal Society Interface*, vol. 15, no. 143, p. 20170937, 2018.
- [11] A. Mertan and N. Cheney, “Investigating premature convergence in co-optimization of morphology and control in evolved virtual soft robots,” in *European Conference on Genetic Programming (Part of EvoStar)*. Springer, 2024, pp. 38–55.
- [12] T. F. Nygaard, C. P. Martin, E. Samuelsen, J. Torresen, and K. Glette, “Real-world evolution adapts robot morphology and control to hardware limitations,” in *Proceedings of the Genetic and Evolutionary Computation Conference*, 2018, pp. 125–132.
- [13] K. Sims, “Evolving 3d morphology and behavior by competition,” *Artificial life*, vol. 1, no. 4, pp. 353–372, 1994.
- [14] H. Lipson and J. B. Pollack, “Automatic design and manufacture of robotic lifeforms,” *Nature*, vol. 406, no. 6799, pp. 974–978, 2000.
- [15] N. Cheney, R. MacCurdy, J. Clune, and H. Lipson, “Unshackling evolution: evolving soft robots with multiple materials and a powerful generative encoding,” *ACM SIGEVOLUTION*, vol. 7, no. 1, pp. 11–23, 2014.
- [16] A. Eiben and E. Hart, “If it evolves it needs to learn,” in *Proceedings of the 2020 Genetic and Evolutionary Computation Conference Companion*, 2020, pp. 1383–1384.
- [17] J. Luo, A. C. Stuurman, J. M. Tomczak, J. Ellers, and A. E. Eiben, “The effects of learning in morphologically evolving robot systems,” *Frontiers in Robotics and AI*, vol. 9, p. 797393, 2022.
- [18] N. Cheney, J. Bongard, V. SunSpiral, and H. Lipson, “On the difficulty of co-optimizing morphology and control in evolved virtual creatures,” in *Artificial life conference proceedings*. MIT Press One Rogers Street, Cambridge, MA 02142-1209, USA journals-info ..., 2016, pp. 226–233.
- [19] N. Ay, R. Der, and M. Prokopenko, “Guided self-organization: perception–action loops of embodied systems,” *Theory in Biosciences*, vol. 131, no. 3, pp. 125–127, 2012.
- [20] J. Liu, D. Wang, Q. Tian, and Z. Chen, “Learn goal-conditioned policy with intrinsic motivation for deep reinforcement learning,” in *Proceedings of the AAAI conference on artificial intelligence*, vol. 36, no. 7, 2022, pp. 7558–7566.
- [21] S. C. Smith and J. M. Herrmann, “Homeokinetic reinforcement learning,” in *IAPR International Workshop on Partially Supervised Learning*. Springer, 2011, pp. 82–91.

- [22] —, “Evaluation of internal models in autonomous learning,” *IEEE Transactions on Cognitive and Developmental Systems*, vol. 11, no. 4, pp. 463–472, 2018.
- [23] S. Forestier, R. Portelas, Y. Mollard, and P.-Y. Oudeyer, “Intrinsically motivated goal exploration processes with automatic curriculum learning,” *Journal of Machine Learning Research*, vol. 23, no. 152, pp. 1–41, 2022.
- [24] D. J. Hejna, P. Abbeel, and L. Pinto, “Task-agnostic morphology evolution,” in *9th International Conference on Learning Representations, ICLR 2021*, 2021.
- [25] A. S. Klyubin, D. Polani, and C. L. Nehaniv, “Empowerment: A universal agent-centric measure of control,” in *2005 IEEE congress on evolutionary computation*, vol. 1. IEEE, 2005, pp. 128–135.
- [26] R. Der and G. Martius, *The playful machine: theoretical foundation and practical realization of self-organizing robots*. Springer Science & Business Media, 2012, vol. 15.
- [27] L. Le Goff and E. Hart, “Improving efficiency of evolving robot designs via self-adaptive learning cycles and an asynchronous architecture,” in *Proceedings of the Genetic and Evolutionary Computation Conference Companion*, 2024, pp. 1607–1615.
- [28] K. O. Stanley, “Compositional pattern producing networks: A novel abstraction of development,” *Genetic programming and evolvable machines*, vol. 8, pp. 131–162, 2007.
- [29] L. K. Le Goff, E. Buchanan, E. Hart, A. E. Eiben, W. Li, M. De Carlo, M. F. Hale, M. Angus, R. Woolley, J. Timmis, *et al.*, “Sample and time efficient policy learning with cma-es and bayesian optimisation,” in *Artificial Life Conference Proceedings 32*. MIT Press One Rogers Street, Cambridge, MA 02142-1209, USA journals-info ..., 2020, pp. 432–440.
- [30] E. Buchanan, L. K. Le Goff, W. Li, E. Hart, A. E. Eiben, M. De Carlo, A. F. Winfield, M. F. Hale, R. Woolley, M. Angus, *et al.*, “Bootstrapping artificial evolution to design robots for autonomous fabrication,” *Robotics*, vol. 9, no. 4, p. 106, 2020.
- [31] M. Angus, E. Buchanan, L. K. Le Goff, E. Hart, A. E. Eiben, M. De Carlo, A. F. Winfield, M. F. Hale, R. Woolley, J. Timmis, *et al.*, “Practical hardware for evolvable robots,” *Frontiers in Robotics and AI*, vol. 10, p. 1206055, 2023.